

Modeling of natural convection heat transfer

By S. Tieszen, A. Ooi, P. Durbin AND M. Behnia

Results from two-dimensional calculations using the $v^2 - f$ and a $k - \epsilon$ model are compared with data for two geometries, the vertical flat plate and the 5:1 height:width box with a constant temperature hot and cold side wall. The results show that the $v^2 - f$ model is at least as good as a $k - \epsilon$ model with a two-layer wall treatment. The nature of buoyancy/turbulence coupling is discussed, and three different treatments of it are compared. Preliminary results show that all three treatments have little effect on the heat transfer in fully turbulent conditions but that the generalized gradient diffusion hypothesis can make a large difference in the location of transition with the $v^2 - f$ model.

1. Introduction

The progress reported in this study is part of a continuing effort to explore the predictive capability of the $v^2 - f$ elliptic relaxation approach (c.f. Durbin 1991, Durbin 1993, and Lien & Durbin 1996) as a wall treatment. Of particular interest to the current study is the determination of the usefulness of the $v^2 - f$ approach in predicting heat transfer in flows in which buoyancy plays a large role. The $v^2 - f$ approach has proven useful in predicting heat transfer in forced convective flows (Durbin 1993, Behnia *et al.* 1996, 1997).

The prediction of heat transfer in buoyancy influenced flows is important for a number of engineering applications, including cooling of electronics, heating and cooling of buildings, process heat transfer (e.g., heat exchangers), and safety applications (e.g., heat transfer from fires). In many of these applications, mixed convection exists in which both forced and free convection contribute to the heat transfer. As a precursor to attempting the complexities of mixed convection heat transfer, the current study will focus on heat transfer in purely buoyant flows. However, since our ultimate objective is mixed convection, we will limit our scope of natural convection to those scenarios that are associated with some definable average mean flow. Thus, we will not look at turbulent natural convection in boxes that are uniformly heated from below.

Buoyant flows differ from forced convective flows in some significant aspects. In particular, in subsonic forced convective flows, the coupling between the momentum and energy equations tends to be one-way with momentum affecting the advection term in the energy equation. The energy equation typically does not feed back into the momentum equation directly. In buoyant flows, the coupling is direct and two-way with the density gradient in a gravity field appearing in the momentum equations. There is little disagreement about the effect of buoyancy on the mean flow.

On the other hand, the nature of the coupling between buoyancy and turbulence generation is a matter of considerable speculation (Tieszen *et al.* 1996). Take a vertical plume as an example. Vortex dynamicists tend to view buoyancy in terms of baroclinic vorticity generation (BVG). BVG is proportional to the density gradients that are normal (perpendicular) to the pressure gradients. Hence, in a gravitational field, temperature gradients perpendicular to gravity (i.e., horizontal) tend to result in generation of vorticity. The resulting vorticity field is the gradient of velocity in which the hot fluid rises and is replaced by transverse inflow. The interaction of these vortical structures is chaotic and turbulence results. In the more traditional perspective, density gradients produce vertical momentum. Conservation of mass requires a transverse inflow to replace the vertically accelerating low-density (high temperature) fluid. Large-scale instabilities occur as the flow accelerates and a turbulent cascade results.

In either view, turbulence is not a direct result of buoyancy, but of instabilities (traditional view) or chaotic interactions among vortical structures (vortex dynamics view). The fundamental question underlying the effect of buoyancy on turbulence is at what length scales does buoyancy express itself. If buoyancy expresses itself at the global length scales, then it need only be represented in the mean flow equations. If buoyancy is responsible (in part) for the large-scale instabilities, then perhaps its coupling to the turbulence is present but weak since flow instabilities will result in a cascade independent of buoyancy. On the other hand, if buoyancy produces small-scale instabilities (or vortical structures, depending on your viewpoint) then the buoyancy-produced structures interact directly with the existing turbulence and the coupling may be strong. The length scales over which buoyancy expresses itself are not currently well understood. Hence, the difficulty in modeling their interaction with turbulent momentum.

Turbulence expresses itself in the Reynolds Averaged Navier Stokes (RANS) equations as long time or ensemble averages of unresolved temporal fluctuations. In the mean flow equations, these are the Reynold stresses in the momentum equations, $\rho \langle u_i u_j \rangle$, and turbulent flux in the energy equation, $\rho \langle u_i h \rangle$. In either case, buoyancy does not change this result, i.e., the buoyant term is linear so does not show up as a non-linear cascade requiring an independent closure term. In RANS modeling, buoyant-turbulence interaction expresses itself as a production term in the turbulence equations. In the context of the current study, this is in the k , ϵ , and f equations. Therefore, in the current modeling strategy, the buoyancy/turbulence interaction question becomes one of modeling the production term in these equations.

Hanjalic (1994) gives a good overview of the different levels of buoyancy modeling that have been attempted. He begins with a second order closure and shows successive simplifications that can be made through algebraic stress models to models compatible with $k - \epsilon$ level approaches. To represent flows without a steady mean flow, such as the bottom heated box, it is necessary to include temperature fluctuations as a source term. Hence a transport equation for temperature variance and, in some cases, its dissipation need to be modeled. Since this set of problems is beyond

the current study's interest, simpler closures (simple and generalized gradient) will be adopted as well as leaving the buoyancy only in the mean flow equations. This approach is more recently justified by the DNS study of Boudjemadi *et al.* (1998). For studying heat transfer, the velocity and temperature gradients in the near wall region are important. The velocity profile in a natural convection boundary layer is somewhat similar to a wall jet (Tsuji & Nagano 1988). However, the natural convection boundary layer has an interesting feature in the near wall region not found in momentum driven flows. From the wall to the velocity maximum, buoyant production offsets viscous production of u_1u_2 so that in the near wall region the absolute value of u_1u_2 is lower than would be found in a wall jet – nearly zero. As a result, u_1u_2 is not correlated well with the mean velocity gradient ($\partial U/\partial x_2$). Hence the gradient diffusion approximation for momentum (eddy viscosity) breaks down in this region. The gradient diffusion approximation is still good for the turbulent thermal flux, however, in the same region. In the outer flow, from the velocity peak outward, the turbulence values are similar to those in a wall jet. This near wall feature indicates that buoyancy does have an effect on the turbulence at small length scales, sufficiently strong to cause a qualitative difference in the flow.

Since the near wall region is important to heat transfer, it has been found that the wall treatment is very important to modeling the heat transfer (Ince & Launder 1989, Henkes 1990, Henkes & Hoogendoorn 1989, 1995). For example, Henkes (1990) found that for a hot plate at $Ra = 10^{11}$, standard $k - \epsilon$ without a wall treatment resulted in a prediction 52% over experimental values. With the wall treatments he tried, the discrepancy was about $\pm 17\%$.

Therefore, even though the $v^2 - f$ approach for wall treatments has proven successful, because of the physical differences between buoyant flow and forced convection flows, and the sensitivity of heat transfer to wall treatments, it is necessary to test the $v^2 - f$ model in these flows. Two standard test cases were chosen and will be discussed in the next section. The models and numerics will be discussed following the description of the test cases, followed by results and conclusions.

2. Benchmark problems

Two benchmark problems, shown schematically in Fig. 1, were chosen: the first is the heated vertical plate; the second is the hot wall - cold wall box. These flows have been studied both experimentally and numerically. As a consequence, comparisons can be made with both the data and other models.

There are two difficulties with buoyant flows that affect to one degree or another all the data. The first difficulty is that purely buoyant flows that have been studied experimentally undergo a laminar to turbulent transition (other than the box heated from below). Transition is not a challenge experimentally, but computationally it is difficult because of the complex physics and small scale structures involved. In the boundary layer problem, numerical transition is usually handled by artificially tripping the boundary layer at the experimentally determined location. However, in the box problem, which is elliptic in nature, it is difficult to artificially trip the solution. Therefore, the comparison is complicated by uncertainties in both the

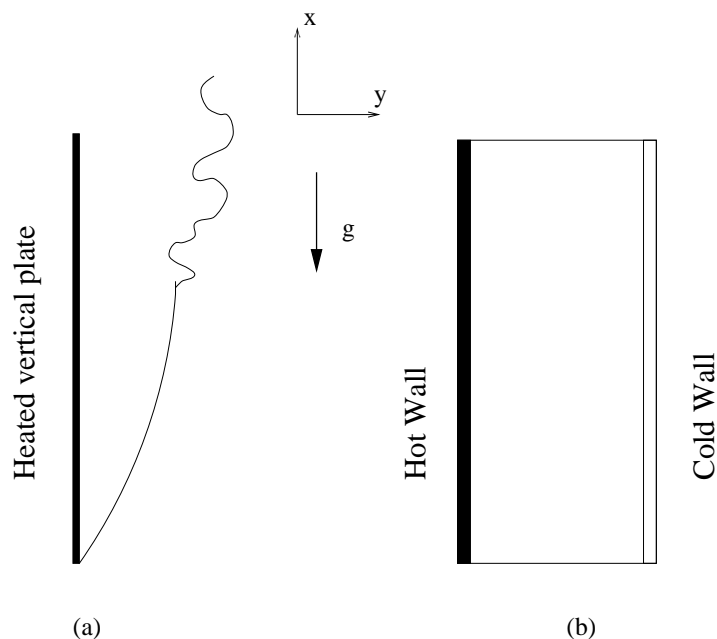


FIGURE 1. Benchmark problems for comparison with $v^2 - f$ results. (a) is a schematic of the vertical flat plate boundary layer problem and (b) is the heated rectangular box.

turbulent heat transfer prediction and the location of transition, which strongly affects the flow pattern.

The second difficulty with natural convection flows is that they are generally low velocity (low momentum) and coupled into the energy equation so they are difficult to stabilize into a prescribed flow pattern. The experimental studies selected for benchmarks all attempted to produce two-dimensional flow patterns so as to facilitate comparison with numerical data. It has proved particularly difficult to produce a truly two-dimensional flow in the box geometry. Numerically, the low momentum and tight coupling with the energy equation expresses itself in long iteration times to reach steady state.

The heated vertical plate is the simplest canonical flow for buoyant heat transfer. As such it has been studied experimentally by a number of investigators including Warner & Arpaci (1968), Cheesewright (1968), Pirovanov *et al.* (1970), Siebers, Schwind & Moffat (1983), and Tsuji & Nagano (1988a, 1988b). Numerical simulations of the heated plate include Lin & Churchill (1978), Henkes & Hoodendoorn (1989), and Peeters & Henkes (1992).

The hot wall - cold wall box is more complex than the boundary layer in that it has a temperature gradient along the vertical centerline and adverse pressure gradients as the flows approach the corners. Data for box geometries include Cheesewright, King & Ziai (1986), Cheesewright & Ziai (1986) and King (1989) for a 5:1 vertical to horizontal aspect ratio and Betts & Bokhari (1995) and Dafa'Alla & Betts (1996) for a 28.6:1 aspect ratio. Numerical simulations of the hot wall - cold wall box include Henkes & Hoogendoorn (1995) for the 5:1 box and Bassina *et al.* (1998),

for the 28.6:1 aspect ratio.

3. Computational models

For the problems studied, variable density was allowed only in the buoyancy term (Boussinesq approximation). With this simplification, the RANS mean-flow equations are:

$$\frac{\partial}{\partial t}(\rho U_i) + \frac{\partial}{\partial x_j}(\rho U_i U_j) = \frac{\partial}{\partial x_j} \left(\mu \left(\frac{\partial U_i}{\partial x_j} + \frac{\partial U_j}{\partial x_i} \right) \right) - \frac{\partial P}{\partial x_i} - g_i \beta (\Theta - \Theta_\infty) + \frac{\partial}{\partial x_j} (-\rho \langle u_i u_j \rangle) \quad (1)$$

$$\frac{\partial}{\partial t}(\rho c_p \Theta) + \frac{\partial}{\partial x_i}(\rho U_i c_p \Theta) = \frac{\partial}{\partial x_i} \left(k \frac{\partial \Theta}{\partial x_i} \right) + \frac{\partial}{\partial x_j} (-\rho c_p \langle u_j \theta \rangle) \quad (2)$$

where $\langle \rangle$ denote ensemble averaging. Θ and θ are the mean temperature and its fluctuating part respectively. All other symbols have their usual meaning. For the vertical flat plate, the standard boundary layer approximations are used and the parabolic equations are solved.

For the momentum equations, the Reynold stress term $\langle u_i u_j \rangle$ is closed with the usual simple gradient assumption.

$$\rho \langle u_i u_j \rangle = \rho \left(\frac{2}{3} \right) k \delta_{ij} - \mu_t \left(\frac{\partial U_i}{\partial x_j} + \frac{\partial U_j}{\partial x_i} \right) \quad (3)$$

This assumption is made for convenience only. The data of Tsuji & Nagano (1988b) show that from y^+ of about 20 to 100 that $\langle u_1 u_2 \rangle$ is not correlated with the mean velocity gradient (in this paper 1 & 2 are the streamwise and cross-stream indices respectively). To correctly model this trend in the data, a more general algebraic or second order closure model for momentum would be required (Peeters & Henkes 1992). It may be expected that ignoring this trend will produce a difference in the calculated skin friction. However, for this study, we will assume that the effect of modeling the momentum transfer in the boundary layer with the simple gradient diffusion approximation will have little effect on the heat transfer predicted. To validate this assumption, comparison with experimental data must be made.

The $v^2 - f$ model of Durbin (1995) is used to obtain the eddy viscosity and provide a wall treatment. The eddy viscosity is given by:

$$\mu_t = \rho C_\mu v^2 T \quad (4)$$

where k , ϵ , v^2 , and f are given by the solutions of

$$\frac{\partial v^2}{\partial t} + U_j \frac{\partial v^2}{\partial x_j} = k f - v^2 \frac{\epsilon}{k} + \frac{\partial}{\partial x_j} \left[\left(\nu + \frac{\nu_t}{\sigma_k} \right) \frac{\partial v^2}{\partial x_j} \right] \quad (5)$$

$$L^2 \frac{\partial^2 f}{\partial x_j \partial x_j} - f = (1 - C_1) \frac{[(2/3) - v^2/k]}{T} - C_2 \frac{P}{k} \quad (6)$$

$$\frac{\partial k}{\partial t} + U_j \frac{\partial k}{\partial x_j} = P - \epsilon + \frac{\partial}{\partial x_j} \left[\left(\nu + \frac{\nu_t}{\sigma_k} \right) \frac{\partial k}{\partial x_j} \right] \quad (7)$$

$$\frac{\partial \epsilon}{\partial t} + U_j \frac{\partial \epsilon}{\partial x_j} = \frac{C_{\epsilon_1} P - C_{\epsilon_2} \epsilon}{T} + \frac{\partial}{\partial x_j} \left[\left(\nu + \frac{\nu_t}{\sigma_\epsilon} \right) \frac{\partial \epsilon}{\partial x_j} \right], \quad (8)$$

with time and length scales given by

$$L^2 = C_L \max \left[\frac{k^3}{\epsilon^2}, C_\eta^2 \left(\frac{\nu^3}{\epsilon} \right)^{1/2} \right] \quad (9)$$

$$T = \max \left[\frac{k}{\epsilon}, 6 \left(\frac{\nu}{\epsilon} \right)^{1/2} \right]. \quad (10)$$

The model constants are

$$\begin{aligned} C_\mu &= 0.22, C_{\epsilon_2} = 1.9, C_1 = 1.4 \\ C_2 &= 0.3, C_L = 0.3, C_\eta = 70 \end{aligned} \quad (11)$$

$$\sigma_k = 1.0, \sigma_\epsilon = 1.3$$

In Eqs. (6), (7), and (8) the production term is given by

$$P = \nu_t \left(\frac{\partial U_j}{\partial x_i} + \frac{\partial U_i}{\partial x_j} \right) \frac{\partial U_j}{\partial x_i} + G \quad (12)$$

where G is the buoyant production term and will be subject to several treatments as described below.

The standard $k - \epsilon$ model is given by Eqs. (7) & (8) with time scale $T = k/\epsilon$. The buoyant production term is not included in the ϵ equation (Eq. (8)). The eddy viscosity is given by

$$\mu_t = \rho C_\mu \frac{k^2}{\epsilon} \quad (13)$$

The two-layer wall treatment is the one-equation model of Wolfstein (1969). In the inner layer where

$$Re_y = \frac{k^{1/2} y \rho}{\mu} < 200,$$

the eddy viscosity is given by

$$\mu_t = \rho C_\mu k^{1/2} l_\mu \quad (14)$$

and

$$\epsilon = \frac{k^{3/2}}{l_\epsilon} \quad (15)$$

$$l_\mu = c_l y \left(1 - \exp\left(-\frac{Re_y}{A_\mu}\right) \right) \quad (16)$$

$$l_\epsilon = c_l y \left(1 - \exp\left(-\frac{Re_y}{A_\epsilon}\right) \right) \quad (17)$$

The constants used to simulate this model can be found in Chen & Patel (1988).

Specification of the turbulent thermal flux is required to close the mean energy equation (Eq. (2)). In the current study, $\langle u_i \theta \rangle$ is closed by the simple mean gradient assumption consistent with the eddy viscosity closure for momentum. The ratio of turbulent to thermal eddy viscosity is the turbulent Prandtl number, Pr_t . Its value is 0.9 for the current study. The closure term is

$$\langle u_i \theta \rangle = -\frac{\nu_t}{Pr_t} \frac{\partial \Theta}{\partial x_i} \quad (18)$$

Tsuji & Nagano (1988b) show that the cross-stream thermal flux is correlated with the mean cross-stream temperature gradient (i.e., it remains positive with a negative temperature gradient) for a large part of the boundary layer. The turbulent Prandtl number ranges from 0.9 to about 1.1 before it becomes ill defined from the velocity peak to the wall, suggesting that this assumption might not be valid in the inner region of the boundary layer.

In keeping with the uncertainty in the physical coupling of buoyancy and turbulence, several treatments are employed to close the buoyant production term in Eqs. (6), (7), and (8). In all cases, the buoyant production term is given by,

$$G = -\beta g \langle u_1 \theta \rangle, \quad (19)$$

where β is the thermal expansion coefficient. $\beta = 1/T$ for the cases studied here (air as the fluid).

In the first level of treatment, G is set equal to zero. This level of treatment is consistent with the assumption that buoyancy affects only the global length scales of the problem and expresses itself in turbulence only through velocity gradients that produce the Reynold stresses.

The second level of treatment is to employ the simple gradient diffusion approximation for $\langle u_i \theta \rangle$ consistent with the approximations used in the mean flow equations. This approximation gives

$$G = -\frac{g}{T} \frac{\nu_t}{Pr_t} \frac{\partial \Theta}{\partial x_1} \quad (20)$$

This approximation is the most common, and perhaps its use is more for consistency of approximation in all equations than in its physics representation. In Eq. (20), the production term is proportional to the temperature gradient in the direction

of gravity. Therefore, this mechanism only allows buoyancy to be represented by streamwise temperature gradients. In stratified flows, clearly the vertical temperature gradient will affect the flow (Rodi 1987). However, Eq. (20) suggests that stratification strongly affects the length scale at which buoyancy expresses itself. If the flows are not stratified, then buoyancy expresses itself only in the mean flow equations (global problem length scales). If it is stratified, then buoyancy expresses itself in turbulent production (length scales within the turbulent spectrum). Typically, the vertical stratification in many flow situations is small compared to cross-stream gradients such as in the problems studied here. It is not clear how shallow vertical temperature gradients could reduce the scale of the buoyant instabilities to create turbulent production, yet sharp horizontal gradients express themselves only at global problem length scales (i.e., no production from cross-stream derivatives).

The third level of treatment is to employ the generalized gradient diffusion approximation (Daly & Harlow 1970 and Ince & Launder 1989) for $\langle u_i \theta \rangle$. This is the simplest closure known to the authors for which temperature gradients perpendicular to gravity result in buoyant production. The generalized gradient diffusion hypothesis (GGDH) is

$$G = -g_i \beta c_\theta \frac{k}{\epsilon} \langle u_i u_j \rangle \frac{\partial \Theta}{\partial x_j}, \quad (21)$$

with the Reynold stresses given by Eq. (3). In the boundary layer implementation, the streamwise derivatives are dropped.

For the vertical plate, a parabolic marching solver is used. The first mesh point is located at $y^+ \approx 1$, with 200 mesh points in the cross-stream direction. The mesh is not evenly distributed, but stretched in the cross-stream direction using a hyperbolic tangent function. For selected calculations, the mesh was doubled and no significant changes were found. For the box problem, a commercial code (FLUENT 4.4) is used. The solver employed uses the SIMPLE algorithm and the QUICK second order interpolation scheme. The first mesh point was located at $y^+ = 5$ with a 150×150 mesh grid. The mesh is not evenly distributed. Fine mesh is used close to the wall and gets coarser towards the center plane of the box. For selected cases, a 75×75 mesh grid was employed and small changes were noted in the solutions, so subsequent runs were all made at 150×150 .

4. Results

Solutions using the $v^2 - f$ model are compared with experimental data in Figs. 2-4 for the vertical plate benchmark. Figure 2 shows the $v^2 - f$ model and data sets for local Nusselt number versus Rayleigh number, where

$$Ra_x = \frac{g\beta\Delta\Theta x^3 Pr}{\nu^2} = Gr_x Pr \quad (22)$$

and Gr_x is the Grashof number. The calculation used the level 1 treatment for buoyancy, i.e., it was not included in the production terms. The calculation was started with a laminar profile as the inlet boundary condition and marched up

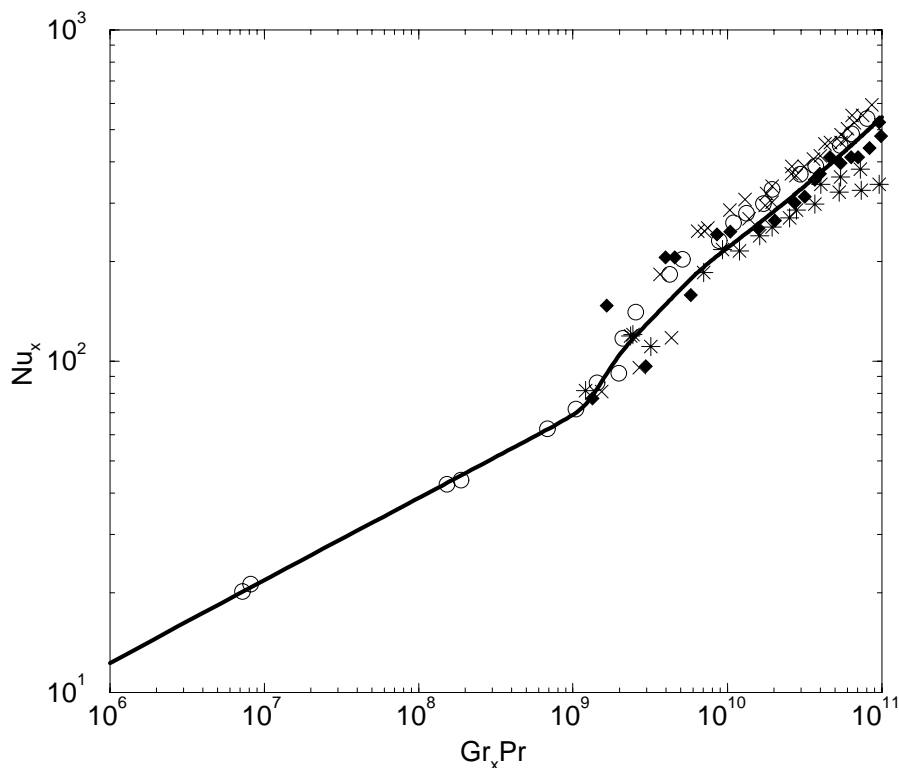


FIGURE 2. Nu_x vs. $Gr_x Pr$ for the vertical flat plate boundary layer. — $v^2 - f$ turbulence model, \times Cheesewright (1968), \blacklozenge Pirvano *et al.* (1970), \circ Tsuji & Nagano (1988), $*$ Warner & Arpaci (1968).

the plate. At $Gr_x \approx 10^9$ the computation was deliberately tripped to turbulence by initializing k , ϵ , and v^2 to some small values, and Eqs. (5)-(8) were solved to simulate the development of the turbulence quantities in the boundary layer.

As is evident from Fig. 2, the $v^2 - f$ turbulence model agrees very well with experimental data. The predictions are well within the scatter of the data from various experiments. Note that the scatter of the data within each experiment is less than between experiments. This error indicates that apparatus/measurement technique dependency (bias error) dominates the uncertainty. Tsuji and Nagano, (1988a), suspect small gradients in the ambient air temperature.

The mean streamwise velocity profiles at various Gr_x are shown in Fig. 3. The $v^2 - f$ model calculation and the experiments of Tsuji & Nagano (1988) are shown. Data have been non-dimensionalized by standard wall units. The $v^2 - f$ calculation used the level 3 treatment for buoyancy. As will be discussed below, little effect was noted for the vertical plate problem for the different buoyancy treatments. The comparison between the $v^2 - f$ model and the data is again very good with the velocity peak predicted in location and amplitude quite closely.

In general, the effect of the different buoyancy treatments was small. Figure 4 shows the comparison of level 1 and level 3 treatments on the thermal eddy viscosity

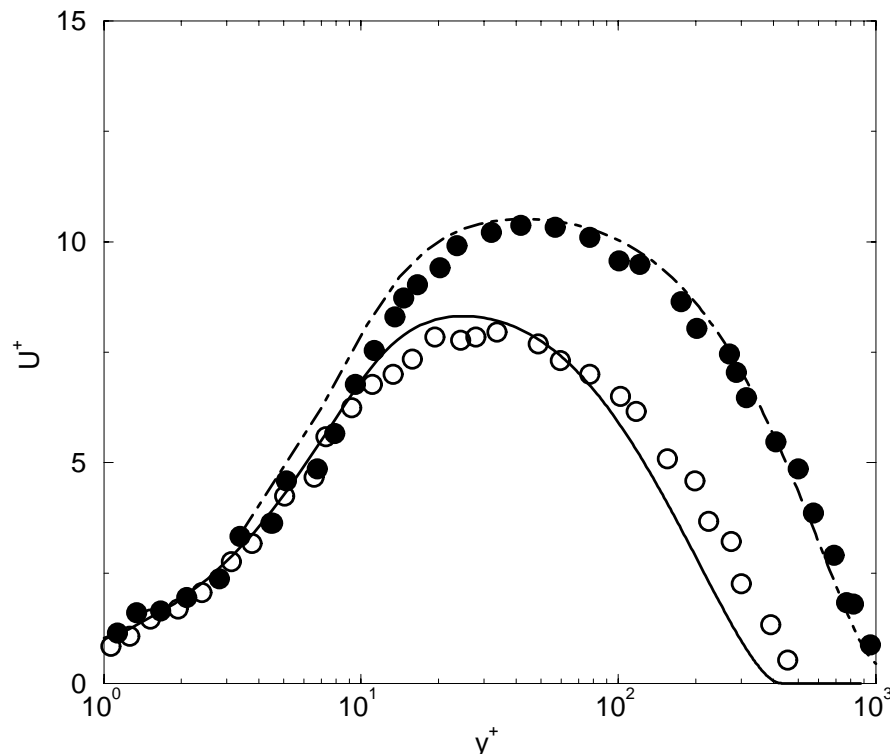


FIGURE 3. U^+ vs y^+ for the vertical flat plate boundary layer. Lines are data from the $v^2 - f$ numerical model (— $Gr_x = 1.56 \times 10^{10}$, --- $Gr_x = 1.80 \times 10^{11}$) and symbols are from experimental data of Tsuji & Nagano (1988a) (\circ $Gr_x = 1.56 \times 10^{10}$, \bullet $Gr_x = 1.80 \times 10^{11}$).

as a function of non-dimensional distance from the wall. The GGDH model has an adjustable constant that was set at 0.05 in Fig. 4. This value is about 1/3 that used by Ince & Launder (1989). Further adjustment upward would result in a better fit of the data in the outer part of the boundary layer from y^+ of 100 to 1000 but would degrade the comparison in the inner part of the boundary layer from y^+ of 25 to 100. As will be noted later, the value at 0.05 resulted in a good comparison with the box data. Hence, the constant was left at 0.05.

The small effect of the three treatments on the results that could be interpreted to mean buoyancy is unimportant as a source of turbulence. However, there is still a significant discrepancy in the thermal eddy viscosity between the $v^2 - f$ results and the data. Another interpretation is that the treatments attempted in this study are insufficient to represent the effects of buoyancy, and perhaps a more general treatment such as proposed by Hanjalic (1994), is required. It was reported by Tsuji & Nagano (1988b) that the eddy viscosity, defined by

$$\nu_t = -\langle uv \rangle / \partial_y U, \quad (23)$$

has an unusual form (going to $\pm\infty$) as a function of y_+ for the thermal boundary

FIGURE 4. Normalized turbulent thermal viscosity vs. y^+ . — standard $v^2 - f$ model, --- $v^2 - f$ model with GGDH and $C_g = 0.05$, \circ Tsuji & Nagano (1988). Data compared at $Gr_x = 9 \times 10^{10}$.

layer. This behavior cannot be represented with a simple gradient diffusion model for eddy viscosity that has been used in the current study.

The $v^2 - f$ model results are compared with data in Figs. 5-8 for the 5:1 vertical box. Figure 5 shows streamlines of the flow in the box from the $v^2 - f$ model with level 1 buoyancy treatment. The flow pattern is basically two separate wall boundary layers that are not interacting. In the experiment by Cheesewright, King & Ziai (1986), it was noted that the effects of the hot and cold walls were not symmetric and that there was re-laminarization as the flow passed across the floor of the cavity followed by a new transition approximately 20% of the way up the hot wall. In Fig. 5, the broadening of the boundary layers just past the mid-height of the box indicated for the level 1 buoyancy treatment that the transition was delayed in the calculation relative to the experiments.

Figure 6 shows the $v^2 - f$ model with two levels of buoyancy treatment (1 and 3), the $k - \epsilon$ model (buoyancy treatment 2) with a two layer wall treatment, and data sets for $Nu_x/Ra_x^{1/3}$ vs. x/H . Comparing the $v^2 - f$ model with level 1 buoyancy and the $k - \epsilon$ model against the hot wall data (King 1989) shows that the heat transfer is slightly underpredicted by the $k - \epsilon$ model and significantly underpredicted by the $v^2 - f$ model. However, the $v^2 - f$ results with GGDH



FIGURE 5. Contours of the stream function.

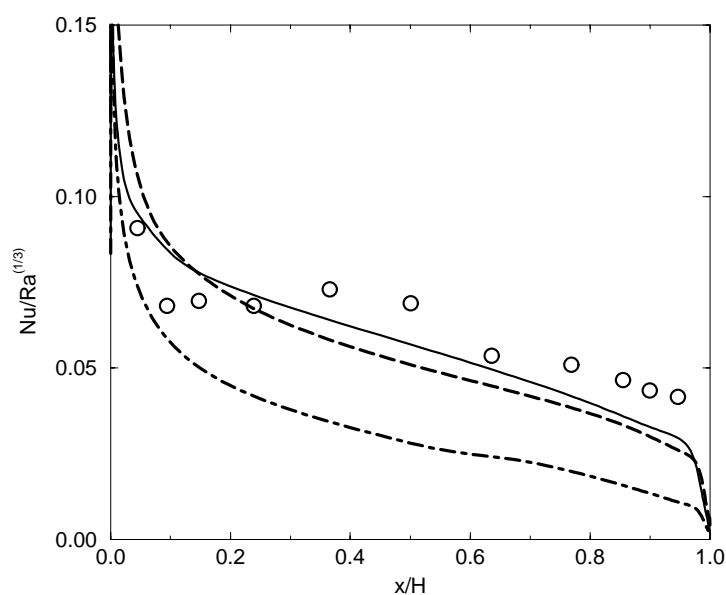


FIGURE 6. This figure shows the local Nusselt number divided by the cube root of the local Rayleigh number vs. non-dimensional height up the wall. \circ Experimental data (King 1989), ---- KEPS (level 2), -.-.- $v^2 - f$ (level 1), — $v^2 - f$ (level 3).

buoyancy treatment provides the best comparison.

The underprediction by the $v^2 - f$ model without the GGDH buoyancy treatment is a result of a late transition to turbulence by the model. This can be seen by the change in slope of the curve around a $y/H = 0.6$. It is seen more clearly in Fig. 7, which shows the vertical velocity distribution in the horizontal (cross-stream) direction. The $v^2 - f$ model with the level 1 treatment has a very narrow distribution, which is characteristic of a laminar boundary layer. With the introduction of the generalized gradient diffusion term (level 3 buoyancy) into the $v^2 - f$ model, the boundary layer transitions much earlier, thus broadening the profile as seen in Fig. 7

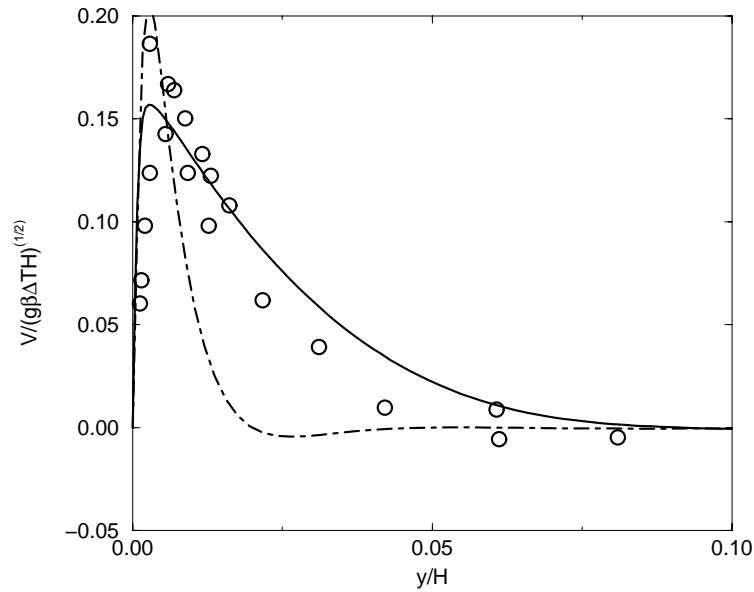


FIGURE 7. Mean vertical velocity profiles at $x = H/2$. \circ Experimental data of Cheesewright (1986), $-\cdot-$ level 1 treatment of the $v^2 - f$ model, $—$ $v^2 - f$ model with GGDH.

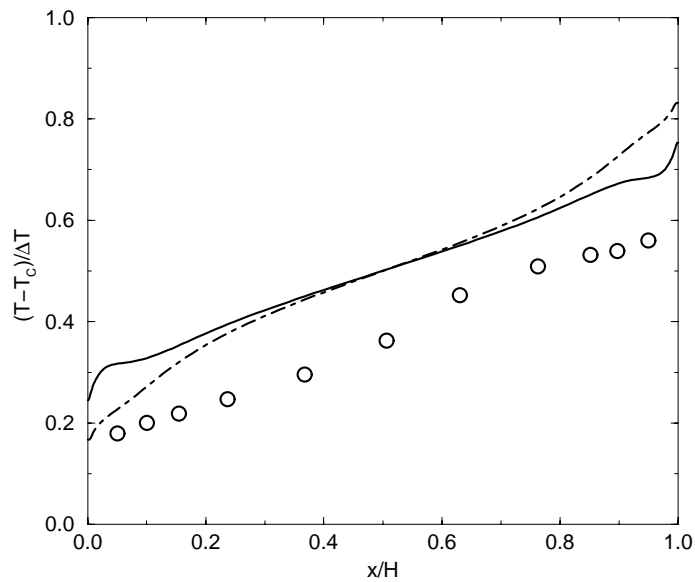


FIGURE 8. This figure shows the $(\Theta - \Theta_c)/\Delta\Theta$ vs. non-dimensional height up the wall. \circ Experimental data (Cheesewright & Ziai, 1986), $—$ $v^2 - f$ model with GGDH, $-\cdot-$ level 1 treatment of the $v^2 - f$ model.

and matching the vertical heat transfer profile much better as seen in Fig. 6.

Experimental data for natural convection in a box is hard to obtain because small amounts of heat loss have a large effect on the outcome. Figure 8 shows the center-plane temperature profile versus elevation. The variables are non-dimensionalized such that at mid-height the temperature should be 0.5. In both calculations it is, but in the data it is lower. This is due to heat loss from the box. In general, the slope of the curve with elevation is better predicted with the $v^2 - f$ model with the level 3 buoyancy treatment than the $v^2 - f$ with level 1 buoyancy treatment.

5. Conclusions

The $v^2 - f$ model compared well with the vertical flat plate data without changes. However, in the hot-wall, cold-wall box, it had a delayed transition with respect to the data and significantly underpredicted the heat transfer. With the addition of the generalized gradient diffusion term to the model, the transition occurred near that in the data and the overall heat transfer comparisons were excellent. Since a coefficient was set in the generalized gradient diffusion term, substantially more comparisons are needed to establish whether or not it is generally useful in transitionally buoyant flows. From the vertical plate data, it seems to have little effect on the heat transfer in fully developed turbulent flows.

The nature of buoyancy/turbulence interactions is not well known. Hence, the ability to model it is not universally agreed upon. Of the three levels of treatment of the buoyant production term tested, none produced any large effect (outside of the location of transition) on the heat transfer. It is not clear whether this outcome means that buoyancy has little effect, or a more sophisticated model is required to delineate the effects. Certainly the good agreement between the models and the test results indicate that if the effect is large, it is being masked by other modeled terms.

REFERENCES

- BASSINA, I. A., LOMAKIN, S. A., NIKULIN, D. A., STRELETS, M. KH. & SHUR, M. L. 1998 Assessment of Applicability of Modern Models of Turbulence for Calculation of Natural-Convection Flows and Heat Transfer. *High Temperature*. **36**(2), 230-238.
- BEHNIA, M., PARNEIX, S. & DURBIN, P. 1996 Simulation of jet impingement heat transfer with the $k - \epsilon - v^2$ model. *Annual Research Briefs*. Center for Turbulence Research, NASA Ames/Stanford University. 3-16.
- BEHNIA, M., PARNEIX, S., & DURBIN, P. 1997 Accurate modeling of impinging jet heat transfer. *Annual Research Briefs*. Center for Turbulence Research, NASA Ames/Stanford University. 149-163.
- BETTS, P. L. & BOKHARI, H. 1995 New experiments on turbulent natural convection of air in a tall cavity. *IMEchE Conference Transactions*. 4th UK National Conference on Heat Transfer. Paper C510/091 213-217.

- BOUDJEMADI, R., MAUPU, V., LAURENCE D., LE. QUERE P. 1998 Budgets of turbulent stresses and fluxes in a vertical slot natural convection flow at Rayleigh $Ra = 10^5$ and 5.410^5 . *Intl. J. of Heat & Fluid Flow*. **18**(1), 70-79.
- CHEESEWRIGHT, R. 1968 Turbulent Natural Convection From a Vertical Plane Surface. *ASME J. Heat Transfer*. **90**, 1-8.
- CHEESEWRIGHT, R., KING, K. J. & ZIAI, S. 1986 Experimental Data for the Validation of Computer Codes for the Prediction of Two-Dimensional Buoyant Cavity Flows. *Proceedings of the ASME Meeting, HTD*. **60**, 75-81.
- CHEESEWRIGHT, R., & ZIAI, S. 1986 Distributions of Temperature and Local Heat-Transfer Rate In Turbulent Natural Convection in a Large Rectangular Cavity. *Proceedings of the 8th International Heat Transfer Conference, San Fransisco*. 1465-1470.
- CHEN, H. C. & PATEL, V. C. 1988 Near-Wall Turbulence Models for Complex Flows Including Separation. *AIAA J.* **26**(6), 641-648.
- DAFA'ALLA, A. & BETTS, P. L. 1996 Experimental Study of Turbulent Natural Convection in a Tall Air Cavity. *Exp. Heat Transfer*. **9**, 15-194.
- DALY, B. J. & HARLOW, F. H. 1970 Transport Equations in Turbulence. *Phys. Fluids*. **13**(11), 2634-2649.
- DURBIN, P. A. 1991 Near-wall turbulence closure modeling without "damping functions". *Theor. & Comp. Fluid Dynamics*. **3**, 1-13.
- DURBIN, P. A. 1993 Application of a near-wall turbulence model to boundary layers and heat transfer. *International J. Heat & Fluid Flow*. **14**, 316-323.
- DURBIN, P. A. 1995 Separated Flow Computations with the $k - \epsilon - v^2$ model. *AIAA J.* **33**(2), 659-664.
- HANJALIC, K. 1994 Achievements and Limitations in Modeling and Computation of Buoyant Turbulent Flows and Heat Transfer. *10th International Heat Transfer Conference*, Brighton, UK.
- HENKES, R. A. W. M. 1990 Natural-Convection Boundary Layers. *Ph. D. Thesis*, Delft University of Technology, Delft, The Netherlands.
- HENKES, R. A. W. M. & HOOGENDOORN, C. J. 1989 Comparison of turbulence models for the natural convection boundary layer along a heated vertical plate. *International J. Heat & Mass Transfer*. **32**(1), 157-169.
- HENKES, R. A. W. M. & HOOGENDOORN, C. J. 1995 Comparison Exercise for Computations of Turbulent Natural Convection in Enclosures. *Numerical Heat Transfer, Part B*. **28**, 59-78.
- INCE, N. Z. & LAUNDER, B. E. 1989 On the computation of buoyancy-driven turbulent flows in rectangular enclosures. *Intl. J. Heat & Fluid Flow*. **10**(2), 110-117.
- KING, K. J. 1989 *Turbulent Natural Convection In Rectangular Air Cavities*. Ph.D. thesis, Queen Mary College, London, UK.

- LIEN, F. S. & DURBIN, P. A. 1996 Non-linear $k-\epsilon-v^2$ modeling with application to high-lift. *Proceedings of the 1996 Summer Program*. Center for Turbulence Research NASA Ames/Stanford University, 5-22.
- LIN, S. J. & CHURCHILL, S. W. 1978 Turbulent Free Convection From A Vertical, Isothermal Plate. *Numerical Heat Transfer*. **1**, 129-145.
- OSTRACH, S. 1953 An Analysis of Laminar Free Convection Flow and Heat Transfer about a Flat Plate Parallel to the Direction of the Generating Body Force. *NACA Report 1111*.
- PEETERS, T. W. J. & HENKES, R. A. W. M. 1992 The Reynolds-stress model of turbulence applied to the natural-convection boundary layer along a heated vertical plate. *Intl. J. Heat & Mass Transfer*. **35**(2), 403-420.
- PIROVANO, A., VIANNAY, S. & JANNOT, M. 1970 Convection Naturelle En Regime Turbulent Le Long D'Une Plaque Plane Vertical. *Proceedings of the 4th International Heat Transfer Conference*, Paris-Versailles, France, 1-12.
- RODI, W. 1987 Examples of Calculation Methods for Flow and Mixing in Stratified Fluids. *J. Geophysical Res.* **92**(C5), 5305-5328.
- SIEBERS, D. L., MOFFAT, R. F. & SCHWIND, R. G. 1985 Experimental, Variable Properties Natural Convection From a Large, Vertical, Flat Surface. *ASME J. Heat Transfer*. **107**, 124-132.
- TIESZEN, S. R., NICOLETTE, V. F., GRITZO, L. A., HOLEN, J. K., MURRAY, D. & MOYA, J. L. 1996 Vortical Structures in Pool Fires: Observation, Speculation, and Simulation, Sandia National Laboratories, Albuquerque, NM. *SAND96-2607*, November.
- TSUJI, T. & NAGANO, Y. 1988a Characteristics of a turbulent natural convection boundary layer along a vertical flat plate. *Intl. J. Heat & Mass Transfer*. **31**(8), 1723-1734.
- TSUJI, T. & NAGANO, Y. 1988b Turbulence measurements in a natural convection boundary layer along a vertical flat plate. *Intl. J. Heat & Mass Transfer*. **31**(10), 2101-2111.
- WARNER, C. Y. & ARPACI, V. S. 1968 An Experimental Investigation of Turbulent Natural Convection in Air along a Vertical Heated Flat Plate. *Intl. J. Heat & Mass Transfer*. **11**, 397-406.
- WOLFSTEIN, M. 1969 The Velocity and Temperature Distribution of One-Dimensional Flow with Turbulence Augmentation and Pressure Gradient. *Intl. J. Heat & Mass Transfer*. **12**, 301-318.